Journal of Materials Chemistry A

Argyrodite sulfide-based superionic conductor synthesized by liquid-phase technique with tetrahydrofuran and ethanol

Journal:	*Journal of Materials Chemistry A*
Manuscript ID	TA-ART-09-2018-009477.R1
Article Type:	Paper
Date Submitted by the Author:	09-Nov-2018
Complete List of Authors:	Yubuchi, So; Osaka Prefecture University, Department of Applied Chemistry Uematsu, Miwa; Osaka Prefecture University, Applied Chemistry Hotehama, Chie ; Osaka Prefecture University, Applied Chemistry Sakuda, Atsushi; Osaka Prefecture University, Department of Applied Chemistry, Graduate School of Engineering Hayashi, Akitoshi; Osaka Prefecture University, Applied Chemistry Tatsumisago, Masahiro; Osaka Prefecture University, Applied Chemistry

Journal Name

ARTICLE

Argyrodite sulfide-based superionic conductor synthesized by liquid-phase technique with tetrahydrofuran and ethanol

Received 00th January 20xx,
Accepted 00th January 20xx

DOI: 10.1039/x0xx00000x

www.rsc.org/

So Yubuchi, Miwa Uematsu, Chie Hotehama, Atsushi Sakuda, Akitoshi Hayashi* and Masahiro Tatsumisago

Sulfide-based solid electrolytes with halide elements are essential components of advanced all-solid-state batteries. Argyrodite crystals are viable candidates as solid electrolytes for realizing all-solid-state batteries. However, a simple and effective route for the synthesis of these solid electrolytes is required. Herein, argyrodite Li_6PS_5Br superionic conductors were synthesized from a homogeneous solution by a liquid-phase technique. The Li_6PS_5Br solid electrolyte was prepared in a shorter synthesis time of one day using tetrahydrofuran and ethanol as compared with the solid-phase method. More importantly, of all the sulfide-based solid electrolytes prepared by liquid-phase techniques, Li_6PS_5Br showed the highest ionic conductivity of 3.1 mS cm^{-1} at 25 °C. The obtained particle size of 1 μm is suitable for application in all-solid-state cells. Moreover, coating electrode active materials with the solid electrolyte using the precursor solution led to a large contact area between the electrode and electrolyte and improved the cell performance. In addition, an infiltration technique into a porous electrode with precursor solution of solid electrolyte is suitable for forming homogenous composite electrodes to improve the cell performance. The all-solid-state cell using the Li_6PS_5Br fine powder with a high conductivity of 1 mS cm^{-1} or more exhibited the reversible capacity of 150 mAh g^{-1}. This technique is effective for the industrial production of solid electrolytes and is applicable to all-solid-state batteries.

INTRODUCTION

All-solid-state lithium-ion batteries are viable alternatives to conventional batteries employing organic electrolytes because of their benefits, i.e., high power density, high energy density, and long-life operation.[1-5] These advantages stem from the great features of inorganic solid electrolytes (SEs), which have a high lithium ion transport number and no-liquid nature. Sulfide-based SEs have become more widespread as essential components of advanced all-solid-state batteries.[6] Sulfide-based SEs can potentially be employed in conjunction with a Li-metal anode[7] and 5V-class high voltage cathode,[8] resulting in high energy and power densities. Sulfide-based SEs also possess high ionic conductivities (>1 mS cm^{-1} at 25 °C)[3,4,9] and good mechanical properties, enabling the formation of an effective interface between solids.[10] Notably, sulfide-based SEs with halide elements have garnered much attention.[11-14]

The synthesis of sulfide-based SEs with organic solvents *via* liquid-phase (LP) processing is a potential new preparation route for developing SEs to realize all-solid-state batteries, where the process is scalable with a relatively short synthesis time and low synthesis temperature. LP synthesis processes can be categorized into two groups: (1) suspension processes and (2) solution processes. In the former, the synthesis of Li_2S-P_2S_5 SEs is conducted using a suspension containing the Li_2S-P_2S_5 precursor and an organic solvent. Organic solvents such as ethers,[15-17] carbonates,[18] esters,[19] and nitriles[20] are typically used. In the latter, the SEs are prepared from a homogenous solution *via* solution-precipitation processes using SEs obtained by solid-state or mechanochemical techniques. Protic solvents such as amides,[21,22] alcohols,[23-25] and water[26] are generally utilized. Both LP techniques are advantageous in terms of their simplicity and ease of synthesis for generating sulfide-based SEs, as well as for the construction of all-solid-state batteries. The most representative synthesis is that of β-Li_3PS_4 using tetrahydrofuran.[15] In the wake of this investigation, the LP syntheses of sulfide-based SEs with various solvents have been reported (see Table 1). For instance, the syntheses of β-Li_3PS_4 with ethylacetate,[19] $Li_7P_3S_{11}$ with acetonitrile,[20] $Li_7P_2S_8I$ with acetonitrile,[14] Li_4PS_4I with 1,2-dimethoxyethan,[27] $Li_{3.25}Ge_{0.25}P_{0.75}S_4$ with hydrazine,[28] Li_6PS_5Br with ethanol,[24] LiI-Li_4SnS_4 with methanol,[25] and Li_4SnS_4 with water[26] have been executed thus far.

To improve the performance of all-solid-state batteries, the ionic conductivity is the most important factor. A few of the LP-synthesized sulfide-based SEs exhibit a conductivity of more than 1 mS cm^{-1};[20] however, there is no report about the LP synthesis of SEs *via* the solution process. The solution process is favorable for obtaining homogenous electrolytes for application to all-solid-state batteries. As candidates for the liquid-phase

*Corresponding author:
Akitoshi Hayashi (Professor)
Department of Applied Chemistry, Graduate School of Engineering,
Osaka Prefecture University,
1-1 Gakuen-cho, Naka-ku, Sakai, Osaka 599-8531, JAPAN
Tel.: +81-72-2549331; Fax.: +81-72-2549334
E-mail address: hayashi@chem.osakafu-u.ac.jp

Electronic Supplementary Information (ESI) available: [details of any supplementary information available should be included here]. See DOI: 10.1039/x0xx00000x

Table 1. Ionic conductivities for sulfide-based solid electrolytes synthesized by suspension and solution-based processes

Reaction state	Electrolyte	Solvent	Conductivity / mS cm^{-1}	Ref.
Suspension	β-Li_3PS_4	THF	0.164	15
	β-Li_3PS_4	EA	0.33	19
	$Li_7P_3S_{11}$	ACN	1.5	20
	$Li_7P_2S_8I$	ACN	0.63	14
	Li_4PS_4I	DME	0.12	27
Solution	LGPS	Hydrazine	0.113	28
	Li_6PS_5Br	Ethanol	0.19	24
	LiI-Li_4SnS_4	Methanol	0.41	25
	Li_4SnS_4	Water	0.15	26
	Li_6PS_5Br	THF-Ethanol	3.1	This work

LGPS: $Li_{3.25}Ge_{0.25}P_{0.75}S_4$, THF: Tetrahydrofuran, EA: Ethyl acetate, ACN: Acetonitrile, DME: 1,2-dimethoxyethane

synthesis of sulfide-based SEs, $Li_7P_3S_{11}$,[4] $Li_{3.25}Ge_{0.25}P_{0.75}S_4$,[9] and argyrodite[13,29-30] crystals are attractive as they offer high lithium-ion conductivities exceeding 1 mS cm^{-1}. Unfortunately, it is difficult to prepare $Li_7P_3S_{11}$ *via* the solution process because protic solvents decompose the P-S-P bonds in the $P_2S_7^{4-}$ unit. In fact, there are only reports on the LP syntheses of SEs with isolated units such as PS_4^{3-} and SnS_4^{4-}.[24-25] Argyrodite sulfide-based SEs are composed of PS_4^{3-}, S^{2-}, and halide anions and lithium cation. In addition, they are thermodynamically stable materials[31] and show high ionic conductivities of 1 mS cm^{-1} or more at room temperature. Therefore, we have focused on argyrodite sulfide-based SEs and previously reported the LP synthesis with ethanol.[23,24] It was possible to prepare argyrodite SEs by employing a homogeneous solution, given that these species are kinetically stable in ethanol. The issues to be addressed are the relatively low ionic conductivities of argyrodite SEs and the multi-step process flow of the mechanochemical and LP techniques. Therefore, the development of an LP technique for the synthesis of argyrodite sulfide-based SEs with high lithium-ion conductivities from the starting materials is required.

Herein, we report the LP synthesis of an argyrodite Li_6PS_5Br SE with ethanol and tetrahydrofuran using a homogeneous solution process. It was possible to synthesize Li_6PS_5Br SE from the staring materials *via* this synthesis process and to shorten the synthetic time to one day as compared with the time required for the solid-phase method. Of all the SEs prepared by LP techniques, the obtained Li_6PS_5Br shows the highest ionic conductivity of 3.1 mS cm^{-1} at 25 °C. The SE has a particle size of about 1 μm and is thus suitable for application in all-solid-state cells. A wide contact area between $LiNi_{1/3}Mn_{1/3}Co_{1/3}O_2$ and the SE was achieved by coating and infiltration techniques, improving the cell performance. Moreover, it was possible to obtain a high capacity of 150 mAh g^{-1} by using the fine Li_6PS_5Br powder.

Experimental Section

Material synthesis

Li_6PS_5Br solid electrolytes (SEs) were synthesized by a multi-step liquid-phase (LP) technique. Li_2S (Mitsuwa Chemical Co., Ltd., 99.9%), P_2S_5 (Aldrich, 99%), and LiBr (Aldrich, 99.9%) were used as the starting materials. The synthesis of Li_6PS_5Br was conducted *via* the following four steps: (1) Li_2S and P_2S_5 with a stoichiometry of 3 to 1 were mixed in super-dehydrated tetrahydrofuran without a stabilizer (THF, Wako). The mixture was stirred overnight. The THF suspension containing the Li_3PS_4 precursor was thus obtained. (2) Li_2S and LiBr (1:1 molar ratio) were dissolved in super-dehydrated ethanol (EtOH, Wako, 99.5%). (3) The THF suspension and the EtOH solution were mixed to obtain the pale green THF-EtOH precursor solution of Li_6PS_5Br. The final molar ratio of Li_2S, P_2S_5, and LiBr was 5:1:2 in the stoichiometric proportion of Li_6PS_5Br. The concentration of Li_6PS_5Br in the THF-EtOH precursor solution was 4.5 wt.%. (4) The precursor solution was dried at 150 °C under vacuum for 3 h to generate a solid powder. To enhance its crystallinity, the solid powder was heat-treated at 550 °C under dry Ar. Hereafter, the Li_6PS_5Br solid samples prepared by the LP technique with heat treatment at x °C are referred to as "LP-x". For comparison, Li_6PS_5Br was synthesized by a mechanochemical (MC) technique.[29] The MC treatment was carried out using a planetary ball mill (Pulveristte 7, Fritsch) with a zirconia pot (45 mL in volume) and 15 zirconia balls (10 mm in diameter) at ambient temperature. The rotational speed was set at 600 rpm and the milling time was 45 h. The prepared powder was heat-treated at 550 °C under dry Ar to obtain "MC-550". All the experimental processes were performed in a glove box under dry Ar. In addition, three other synthesis processes were conducted by the LP technique using ethanol and tetrahydrofuran as a single solvent system. The experimental procedures are expounded in the Supplementary Information (see supplementary Figure S1). The synthesis conditions are summarized in supplementary Table S1.

The Li_6PS_5Br SE-coated $LiNi_{1/3}Mn_{1/3}Co_{1/3}O_2$ (NMC) powder was prepared by a solution process. The EtOH precursor solution was mixed with NMC powder. The obtained slurry was dried at 150 °C under vacuum for 3 h to remove the EtOH and solidify the electrolyte; thus, NMC particles coated with Li_6PS_5Br SE were prepared. The NMC/SE weight ratios were *x*:100-*x* (*x* = 85, 90, 95). In addition, composite electrodes were prepared by mixing NMC with LP-150 or LP-550 using a mortar. Moreover, the infiltrated NMC electrode was prepared based on a previous report.[32] Initially, the preparation of NMC porous electrode was conducted by casting and spreading a slurry of NMC, acetylene black (AB, Denki kagaku kogyo), and polyvinylidene difluoride binder (PVDF, KF1100, Kureha Inc.) with *N*-methyl-2-pyrrolidone (Wako) solvent on a Al current collector, followed by drying at 120 °C on a hot plate. The SE was infiltrated into the NMC porous electrode by dipping the electrode into the THF-EtOH precursor solution. The obtained composite electrode was dried at 150 °C under vacuum to prepare the infiltrated NMC electrode. The weight ratio of NMC, Li_6PS_5Br SE, AB, and PVDF was 82.2:15.3:1.7:0.8. The NMC powder was pre-coated with $LiNbO_3$ to prevent undesirable side reactions.[33]

Material characterization

Crystallographic phase identification was performed using an X-ray diffractometer (SmartLab, Rigaku) with Cu-Kα radiation. Diffraction data were collected in steps of 0.02° over the 2θ range of 5–80° at a scan rate of 4° min^{-1}. X-ray diffraction (XRD) measurements were conducted using an airtight container with a beryllium window to prevent exposure of the sample to air. The computer program RIETAN-FP[34] was used for the Rietveld analysis. To identify the structural units, Raman spectroscopic analysis was carried out with a Raman spectrophotometer (LabRAM HR-800, HORIBA Ltd.) equipped with a 532 nm He-Ne laser. Scanning electron microscopy characterization was carried out using a field-emission scanning electron microscope (FE-SEM, SU8220, Hitachi High-Technologies) with an energy dispersive X-ray spectroscopy system (EDX, EMAXEvolution X-MAX, Horiba Ltd.). A cross-section of the working electrolyte layer with SE-coated NMC was prepared using an ion milling system with an Ar-ion beam (IM4000, Hitachi High-Technologies). Ion milling to obtain a smooth cross-section was conducted for the sample transferred to an Ar-filled vessel to prevent exposure of the samples to air.

Electrochemical characterization

The ionic conductivity of the SE was measured by electrochemical impedance spectroscopy (EIS). The data were collected in the range of 1 MHz to 10 Hz using an impedance analyzer (1260, Solartron), with an applied AC voltage of 10–25 mV. To determine the ionic conductivities of the SEs, three pellet types were prepared: (1) green compacts pressed at 360 MPa at room temperature, (2) green compacts pressed at 720 MPa at room temperature, and (3) sintered bodies obtained by heat treatment at 550 °C under dry Ar. Au current collectors were used to cover the entire surface of both sides of the pellet. The pellet was sealed in a laminate-type pouch cell to prevent exposure of the sample to air. It was difficult to accurately measure resistances of 100 Ω or less because of the influence of inductance due to the equipment setup, causing the estimated resistance and activation energy of the SEs to be lower than the actual value. Thus, the temperature-dependence of the conductivity was measured from the low temperature region of about −30 °C. The temperature was controlled with an ethanol-cooled bath and a constant temperature bath. The cell was held at the specified temperature for two hours to allow the system to reach thermal equilibrium. The lithium-ion migration activation energy was calculated from the slope of the Arrhenius plot. The electronic conductivity was measured *via* the DC polarization technique. The data were collected using a potentio-galvanostat (S-1287, Solartron) with applied DC voltages of 0.4, 0.5, and 1.5 V at 25 °C.

All-solid-state cells (Li-In/75Li_2S·25P_2S_5 (mol%) glass/NMC) were fabricated with the following three kinds of working electrodes, where NMC loading masses are described in parentheses: (1) SE-coated NMC powder (17.7 mg cm^{-2}), (2) the infiltrated NMC electrode obtained by the LP techniques (17.9 mg cm^{-2}), and (3) a mixture of LP-150 or LP-550 and NMC powder (14.7 mg cm^{-2}). 75Li_2S·25P_2S_5 (mol%) glass prepared by the MC technique was utilized as a standard sulfide electrolyte to a separator layer in order to examine the effects of only composite working electrodes on the cell performance. A bilayer pellet consisting of the working electrode and the separator was compressed under 360 MPa of pressure. Indium foil (Furuuchi Chem., 99.999%) and lithium foil (Furuuchi Chem., 99.9%), as counter electrodes, were attached to the other side of the SE separator. All the processes for preparing the cells were performed under dry Ar. Galvanostatic charge–discharge measurements for the all-solid-state cells were conducted using a charge–discharge measuring device (BTS-2004, Nagao Co., Ltd.) at 25 °C under dry Ar. The electrochemical tests were performed at constant current densities of 0.13, 0.26, 0.52, 1.3, 2.6, and 5.2 mA cm^{-2} in the voltage range of 1.9–3.8 V *vs.* Li-In. The same current densities were applied for the charge and discharge measurements.

RESULTS AND DISCUSSION

Electrolyte characterization

Our previous research showed that the argyrodite sulfide-based Li_6PS_5X (X = Cl, Br, I) solid electrolytes (SEs), which were prepared by the mechanochemical technique (MC), could be dissolved into and precipitated from alcohols.[24] However, for practical application, it is necessary to develop a simple process for the synthesis of argyrodite SEs that does not employ the MC technique. Thus, the following reactions employing a bi-solvent system comprising tetrahydrofuran (THF) and ethanol (EtOH) was employed as an improved process:

$$5Li_2S + P_2S_5 + 2LiBr \xrightarrow{THF} 2Li_3PS_4 + 2Li_2S + 2LiBr \xrightarrow{EtOH} 2Li_6PS_5Br$$

For synthesis of the Li_6PS_5Br SE, the THF-EtOH precursor solution was prepared by mixing a suspension of the Li_3PS_4 precursor in THF and a solution of Li_2S and LiBr in EtOH, as shown in Figure 1.

Figure 2a shows the pale green homogeneous THF-EtOH precursor solution containing Li_6PS_5Br. The LP-150 solid powder obtained by drying the solution at 150 °C under vacuum was subjected to the process described in our previous report.[24] In addition, Li_6PS_5Br was heat-treated at 550 °C to obtain LP-550. Figure 2b shows the Raman spectra for the THF-EtOH

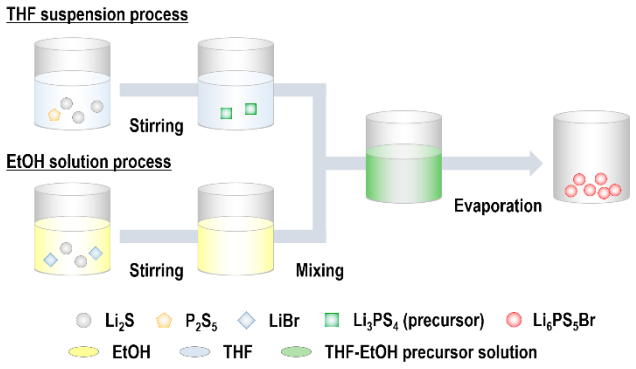

Figure 1. Schematic illustrations of the multi-step LP technique for synthesis of Li_6PS_5Br with both EtOH and THF.

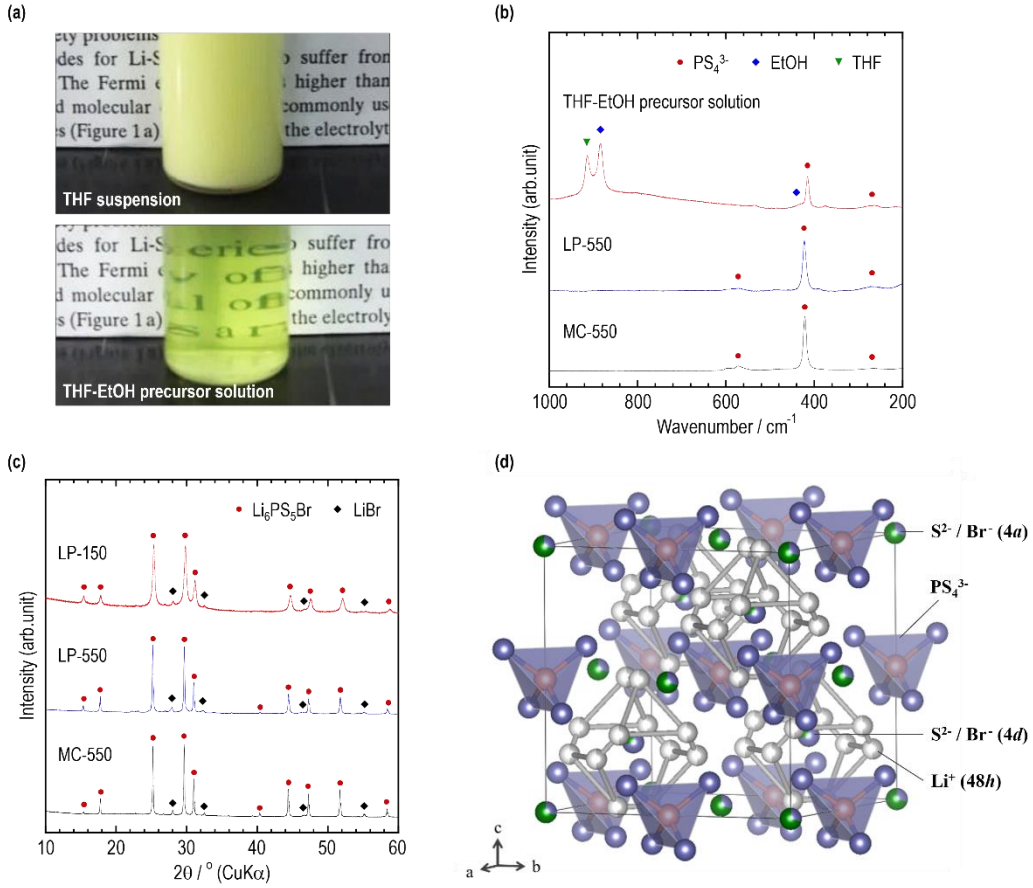

Figure 2. (a) Photographic images of THF suspension of Li_3PS_4 precursor and THF-EtOH precursor solution of Li_6PS_5Br. (b) Raman spectra for THF-EtOH precursor solution of Li_6PS_5Br, LP-550, and MC-550. (c) XRD patterns of LP-150, LP-550, and MC-550. (d) Crystal structure of LP-550 with unit cell outlined. The Li, P, S, and Br sites are represented by gray, orange, purple, and green balls, respectively.

precursor solution containing the Li_6PS_5Br, LP-550, and MC-550 solid powders. In the profile of the THF-EtOH precursor solution, LP-550, and MC-550, strong Raman bands centered around 420 cm^{-1} originating from the PS_4^{3-} unit were detected, indicating that THF and EtOH did not kinetically decompose the PS_4^{3-} unit. The peak of the PS_4^{3-} unit in the Raman profile of the precursor solution was shifted to lower wavenumber. This implies that the PS_4^{3-} unit was solvated with THF and/or EtOH molecules. Such band shifts have also been previously reported.[16] Figure 2c presents the XRD patterns of LP-150, LP-550, and MC-550. All the samples comprised mainly lithium-ion conducting argyrodite Li_6PS_5Br crystals, along with small amount of LiBr crystals. The crystallinity of Li_6PS_5Br was increased by heat treatment at 550 °C. LP-550 was confirmed to have the argyrodite structure (a = 9.9641(2) Å, $F\bar{4}3m$, (216)) from the powder XRD pattern and Rietveld refinement analysis technique (Supplementary Figure S2). The structural parameters are listed in Supplementary Table S2. The parameters are similar to previously reported experimental data.[30] Figure 2d presents the unit cell of Li_6PS_5Br (LP-550), in which the S^{2-} and Br^- anions form a face-centered cubic lattice (Wyckoff positions 4*a* and 4*d*) and PS_4^{3-} tetrahedra on the octahedral sites (P on Wyckoff position 4*b*). Site disorder of the S^{2-} and Br^- anions was observed because of the similar ionic radii of Br^- and S^{2-} anions. The Li^+ site was simply set as the 48*h* site with occupancy of 0.5. The Li^+ sites form a cage-like conduction path and furnish a macroscopically fast conduction pathway. These results are largely similar to those for Li_6PS_5Br prepared by the solid-phase method.[30]

For comparison, Li_6PS_5Br SEs were synthesized from the starting materials (Li_2S, P_2S_5, and LiBr) using either THF or EtOH. With the use of EtOH alone (Supplementary Figure S1a), Li_2S, LiBr, and unknown impurities were formed in addition to Li_6PS_5Br (Supplementary Figure S3a). The Raman spectrum indicates that S-S bonds derived from Li_2S and $P_2S_6^{4-}$ and unknown structural units were generated (Supplementary Figure S3b). This is because P_2S_5 is attacked and decomposed by EtOH.[35] These results show that it is difficult to synthesize single-phase Li_6PS_5Br when EtOH and P_2S_5 are combined. Another process for the synthesis of Li_6PS_5Br with THF alone as a solvent was also examined (Supplementary Figure S1b). The XRD pattern and Raman spectrum show that only Li_2S and P_2S_5 reacted in THF to form Li_3PS_4 (Supplementary Figure S3). This means that argyrodite SEs cannot be synthesized by using THF alone, and the use of both the Li_3PS_4 precursor and EtOH is required to form Li_6PS_5Br. In fact, it was possible to obtain Li_6PS_5Br using $75Li_2S{\cdot}25P_2S_5$ glass prepared by the MC technique (Supplementary Figure S1c, S4, S5, and Table S3). In addition, when only $75Li_2S{\cdot}25P_2S_5$ glass was precipitated from the ethanol solution, the PS_4^{3-} ion was decomposed. Thus, it is

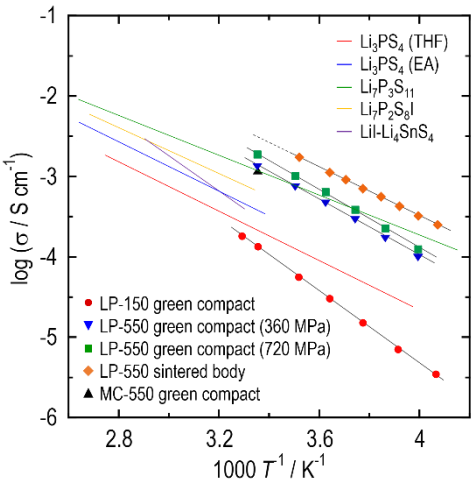

Figure 3. Arrhenius plots of LP-150, LP-550, and MC-550. Green compacts were prepared by pressing at 360 MPa and 720 MPa at room temperature. Sintered body was obtained by heat treatment (at 550°C) of the pellet pressed at 720 MPa. Arrhenius plots of sulfide-based SEs prepared by the LP techniques are also shown[14,15,19,20,25].

considered that excess Li_2S, which is basic, plays an important role in kinetically stabilizing the SEs in the solution.

The ionic conductivities of the obtained Li_6PS_5Br SEs were measured using lithium-ion blocking Au/SE/Au cells by applying electrochemical impedance spectroscopic (EIS) analysis. The temperature-dependence of the conductivity was measured from the low temperature region of about −30 °C (Supplementary Figure S6a). Figure 3 presents the Arrhenius plots of the Li_6PS_5Br SEs prepared by the LP technique (see Table 2 for details). For comparison, the Arrhenius plots of the typical sulfide-based SEs synthesized by other LP techniques[14,15,19,20,25] are also shown (see Supplementary Table S4 for details). The LP-150 green compact pressed at 360 MPa exhibited a conductivity of 0.13 mS cm^{-1} at 25 °C, which is similar to that reported.[24] More importantly, the LP-550 green compact cold-pressed at 720 MPa showed the highest ionic conductivity of 1.9 mS cm^{-1} at 25 °C of all the SEs prepared by the LP techniques. This conductivity is comparable to that of the MC-550 green compact. In addition, the LP-550 green compact showed a much lower electronic conductivity of 4×10^{-8} S cm^{-1} at 25 °C, as measured by the DC polarization technique (Supplementary Figure S6b). The lithium-ion transport number of LP-550 is thus about 1. Moreover, the particle size of LP-550 synthesized by the LP technique is smaller than that of MC-550, as shown in Figure 4. The performance of all-solid-state cells can be improved when a fine SE is used in the composite electrode.[36]

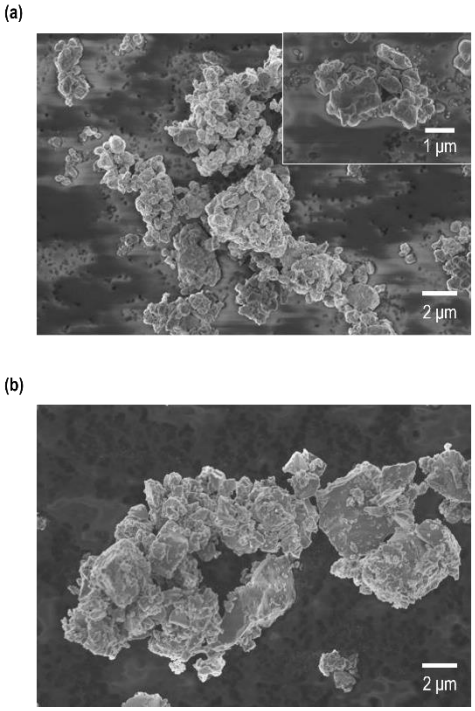

Figure 4. FE-SEM images of (a) LP-550 and (b) MC-550.

However, the ionic conductivity of the green compact of LP-550 was lower than that of the corresponding sintered body because of the greater number of grain boundaries in the green compact; the LP-550 sintered body heat-treated at 550 °C showed the highest conductivity of 3.1 mS cm^{-1} at 25 °C due to a decrease in the grain boundaries during the sintering process (Supplementary Figure S7a and S7b). Conversely, the conductivity of $75Li_2S{\cdot}25P_2S_5$ glass cold-pressed at 360 MPa was as high as that of the hot-pressed counterpart.

The relative density of the green compact tended to be lower for LP-550 (79%) than $75Li_2S{\cdot}25P_2S_5$ glass (90%) at a molding pressure of 360 MPa. The conductivity of the LP-550 green compact increased as the molding pressure increased from 360 MPa to 720 MPa (Supplementary Figure S7b). This improvement is derived from enhancement of the relative density (79% to 86%) given that the activation energies were almost unchanged.

We successfully synthesized a Li_6PS_5Br sulfide-based SE using a homogeneous solution with THF and EtOH *via* only the LP technique. Of all the samples prepared by the LP techniques

Table 2. Ionic conductivities and activation energies of LP-150, LP-550, and MC-550. Green compacts were prepared by pressing at 360 MPa and 720 MPa at room temperature. Sintered body was obtained by heat treatment (at 550°C) of the pellet pressed at 720 MPa.

	LP technique				MC technique
Heat treatment temperature / °C	150	550	550	550	550
Pellet	Green compact	Green compact	Green compact	Sintered body	Green compact
Molding pressure / MPa	360	360	720	720	360
Conductivity at 25 °C / mS cm^{-1}	0.13	1.4	1.9	3.1	1.2
Activation energy / kJ mol^{-1}	42.9	33.8	34.9	29.1	N / A

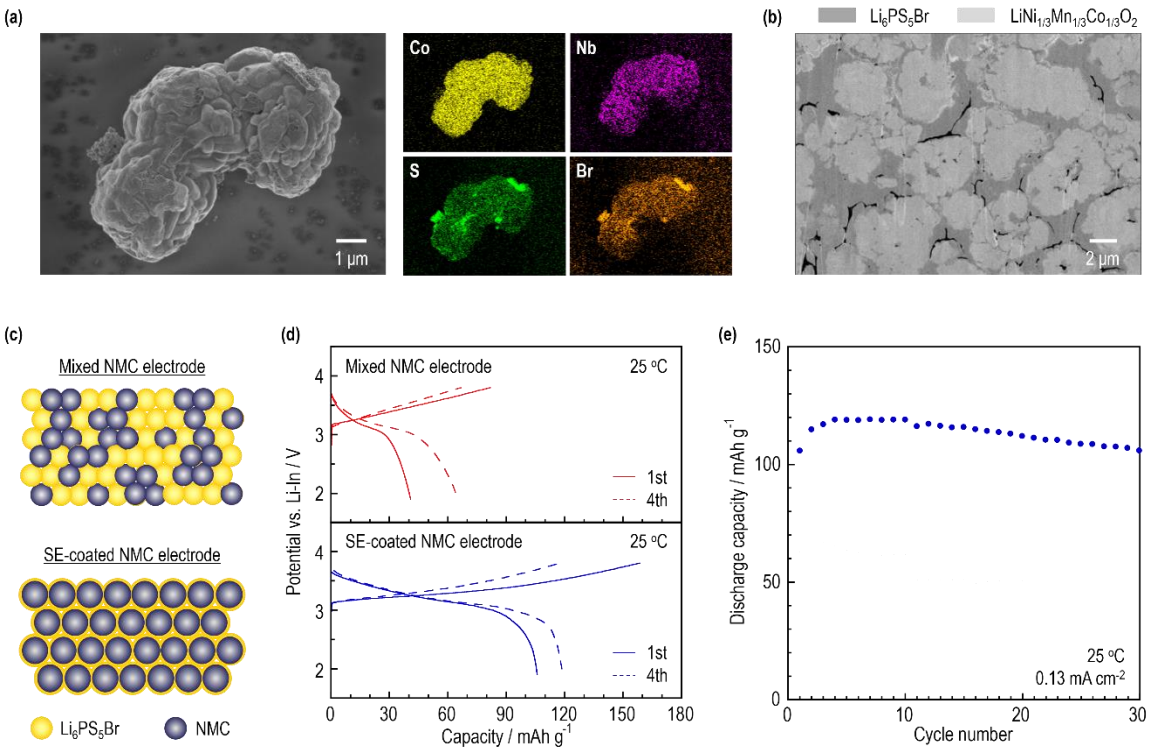

Figure 5. (a) FE-SEM image of SE-coated NMC particles and EDX maps of cobalt, niobium, sulfur, and bromine for the SE-coated NMC particles. (b) Cross-sectional FE-SEM image of the composite positive electrode layer with the SE-coated NMC particles prepared by LP technique. (c) Schematic illustrations of the mixed NMC electrode and the SE-coated NMC electrode. (d) Charge-discharge curves of the cells with the conventional mixed NMC electrode prepared by hand-mixing of NMC and LP-150 particles using a mortar and the SE-coated NMC electrode. (e) Cycle performance of the cell with the SE-coated NMC electrode. The NMC/SE weight ratio was 90:10.

reported so far, Li_6PS_5Br with a small particle size of about 1 μm exhibits the highest ionic conductivity of 3.1 mS cm^{-1} at 25 °C. In addition, it was also possible to synthesize the argyrodite SEs in shorter time of one day compared to seven days required for the existing solid-state method.[13]

Evaluation of all-solid-state cells

Li_6PS_5Br-coated $LiNi_{1/3}Mn_{1/3}Co_{1/3}O_2$ (SE-coated NMC) powder was prepared from an EtOH precursor solution using Li_2S, LiBr, and $75Li_2S{\cdot}25P_2S_5$ glass as the starting materials. The NMC/SE weight ratio was 90:10. NMC particles were covered with the homogenous solution to generate the uniform solid-liquid interfaces, and subsequent removal of the solvent gave close solid-solid interfaces between the NMC particles and SE-coating layer. It has been reported that improved electrochemical performance of all-solid-state cells can be achieved with a homogeneous electrode-electrolyte interface.[37-38] The drying temperature of 150 °C prevents side reactions between the electrode and electrolyte, as described in our previous report.[24] Figure 5a presents the field-emission scanning electron microscopy (FE-SEM) image and energy dispersive X-ray spectroscopy (EDX) maps of cobalt, niobium, sulfur, and bromine for the SE-coated NMC particles. The SE-coating layer covers the uneven surface of the NMC particles. In addition, it is also important that the $LiNbO_3$-coating layer remained on the NMC particles, which prevents undesirable side reactions between electrodes and electrolytes during charging process by physically suppressing the diffusion of the constituent elements.[33,39]

Figure 5b shows the cross-sectional FE-SEM image of the composite positive electrode with SE-coated NMC powder. The cross-sectional image was acquired using FE-SEM with an ion milling system with an Ar-ion beam. The SE layer was observed over almost the entire surface of the NMC particles, indicating that a favorable electrode-electrolyte interface was formed. However, voids were present between the SE-coated NMC particles because the crystalline argyrodite SEs have poor formability compared to $75Li_2S{\cdot}25P_2S_5$ glass, as shown in Figure S7a. To evaluate these-coating effects, two kinds of working electrodes were prepared for the all-solid-state Li-In/Li_3PS_4 glass/NMC cells: (1) SE-coated NMC powders obtained by the LP technique, and (2) a conventional mixture of LP-150 and NMC powder mixed using a mortar (Figure 5c). The NMC/SE weight ratio was 90:10, which is the optimized weight ratio, as shown in Figure S8. Figure 5d presents the charge–discharge curves of the cells, measured at a constant current density of 0.13 mA cm^{-2} in the voltage range of 1.9−3.8 V *vs.* Li-In. The cell with the SE-coated NMC electrode furnished a capacity of 119 mAh g^{-1}, whereas the cell with the mixed NMC electrode produced a capacity of 65 mAh g^{-1} at the 4th discharge process. Despite the use of the same Li_6PS_5Br SE, the cell with the SE-coated NMC electrode exhibited higher capacity than that with the mixed NMC electrode. This is due to the formation of favorable solid-solid electrode-electrolyte interfaces in the SE-coated NMC electrode. The cell with SE-coated NMC also showed stable cycle performance (Figure 5e).

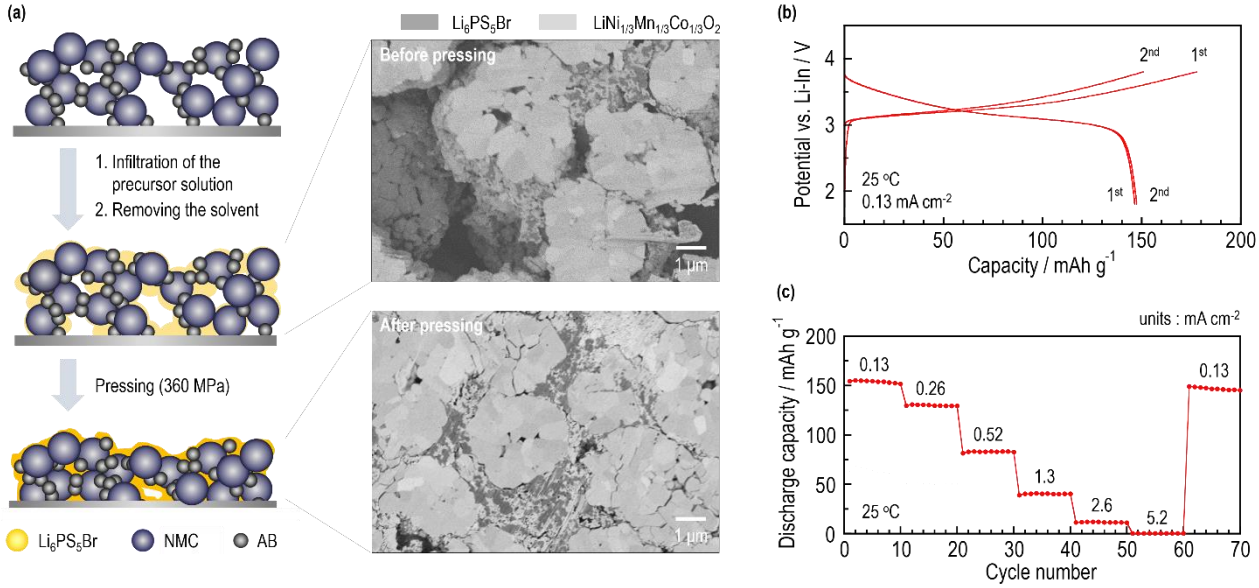

Figure 6. (a) Schematic illustrations of the infiltration process with Li_6PS_5Br SE into a NMC porous electrode by the liquid-phase technique. Cross-sectional FE-SEM images of the infiltrated NMC electrode before (upper image) and after (bottom image) pressing. (b) Charge-discharge curves and (c) rare performance of the cell with the infiltrated NMC electrode. The same current densities were applied for the charge and discharge measurements.

Figure 6a shows schematic illustrations of the infiltration process and cross-sectional SEM images of infiltrated NMC electrodes before and after pressing at 360 MPa. The NMC porous electrode was infiltrated with the THF-EtOH precursor solution of the SE by a capillary force, and then was dried at 150 °C under vacuum. The NMC particles were coated with SE and AB before pressing. Densification by pressing formed favorable electrode-electrolyte interfaces. FE-SEM image and EDX elemental maps for nickel, carbon, and sulfur elements at low magnification (see Figure S9) indicated that the SE was connected over a long distance and favorable conduction pathway was obtained. The cell with the infiltrated NMC electrode was charged/discharged at 25 °C. All-solid-state cell exhibited high reversible capacity of 154 mAh g^{-1} (see Figure 6b). Figure 6c shows the rate and cycle performances. After cycled at higher current densities, the cell operated reversibly with slight capacity deterioration during 10 cycles at the initial current density. From these results, the infiltration with SEs into the porous electrodes is also effective in easily preparing homogeneous composite electrodes to improve the cell performance.

The cell fabricated with the LP-550 electrolyte showed higher conductivity of 1.4 mS cm^{-1}. Unfortunately, SE-coating was not carried out because heat treatment at 550 °C induces side reactions of SE and NMC. Figure 7a shows the cross-sectional FE-SEM image of the mixed NMC electrode with the LP-550 electrolyte. The LP-550 electrolyte and NMC electrode particles formed favorable contacts. The cell with the mixed NMC electrode using the LP-550 electrolyte exhibited a high reversible capacity of 150 mAh g^{-1} at 25 °C, as shown in Figure 7b. This capacity is higher than that of the cell with SE-coated NMC, in which the SE showed lower conductivity. The cell exhibited better rate performance than the cell with the infiltrated NMC electrode (Figure 7c). It is critical to improve the effective ionic

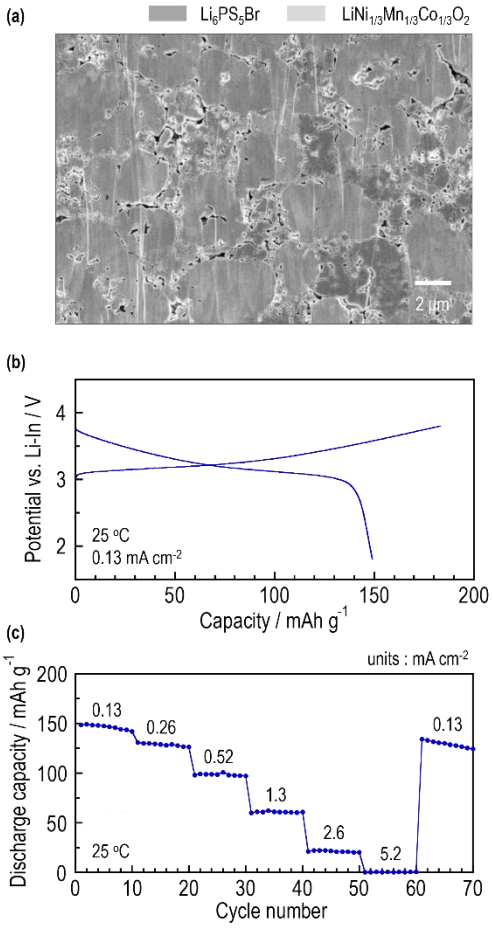

Figure 7. (a) Cross-sectional FE-SEM image of conventional mixed NMC electrode layer prepared by hand-mixing NMC and LP-550 particles using a mortar. (b) Charge-discharge curves and (c) rare performance of cell with conventional mixed NMC electrode. The NMC/SE weight ratio was 80:20. The same current densities were applied for the charge and discharge measurements.

conductivity of the electrode layer, in addition to forming a favorable interface.

We successfully constructed a wide contact area between the NMC electrode and Li_6PS_5Br electrolyte, leading to improved cell performance, by SE-coating and infiltration processes through the LP technique. In addition, the use of a fine Li_6PS_5Br powder exhibiting a higher conductivity of 1 mS cm^{-1} or more further contributed to the improved rate performance.

Conclusions

The sulfide-based superionic conductor, Li_6PS_5Br, was synthesized *via* a liquid-phase technique employing a homogeneous tetrahydrofuran and ethanol-based solution. Synthesis of the Li_6PS_5Br solid electrolyte using tetrahydrofuran and ethanol offers the advantages of a shorter reaction time compared with that of the solid-phase method. Of all the SEs prepared by liquid-phase techniques, the prepared Li_6PS_5Br shows the highest ionic conductivity of 3.1 mS cm^{-1} at 25 °C. In addition, a wide contact area between the NMC electrode and Li_6PS_5Br electrolyte was constructed by the coating technique employing the Li_6PS_5Br precursor solution. This process generated a favorable interface, resulting in a higher reversible capacity of 119 mAh g^{-1} relative to that of the cell with the conventional mixture electrode. In addition, an infiltration technique into a porous electrode with precursor solution of solid electrolyte easily brought about homogenous composite electrodes to improve cell performance. Moreover, the all-solid-state cell employing the fine Li_6PS_5Br powder with a higher conductivity of 1 mS cm^{-1} or more showed a reversible capacity of 150 mAh g^{-1}. Thus, this technique is both effective for the preparation of solid electrolytes and is applicable to all-solid-state batteries.

Conflicts of interest

There are no conflicts to declare.

Acknowledgements

This research was financially supported by the Japan Science and Technology Agency (JST), Advanced Low Carbon Technology Research and Development Program (ALCA), Specially Promoted Research for Innovative Next Generation Batteries (SPRING) project, and by a Grant-in-Aid for Scientific Research from the Ministry of Education, Culture, Sports, Science and Technology of Japan.

Notes and references

1 J.B. Goodenough and Y. Kim, *Chem. Mater*., 2010, ***22(3)***, 587−603.
2 J.-M. Tarascon, *Philos. Trans. R. Soc. A*, 2010, ***368***, 322−3241.
3 Y. Kato, S. Hori, T. Saito, K. Suzuki, M. Hirayama, A. Mitsui, M. Yonemura, H. Iba, and R. Kanno, *Nat. Energy*, 2016, ***1***, 16030.
4 Y. Seino, T. Ota, K. Takada, A. Hayashi, and M. Tatsumisago, *Energy Environ. Sci*., 2014, ***7***, 627–631.
5 A. Hayashi, A. Sakuda, and M. Tatsumisago, *Front. Energy Res*., 2016, ***4***, 25.
6 A.L. Robinson and J. Janek, *MRS Bull*., 2014, ***39***, 1046–1047.
7 M. Nagao, A. Hayashi, and M. Tatsumisago, *Electrochem. Commun*., 2012, ***22***, 177–180.
8 S. Yubuchi, Y. Ito, T. Matsuyama, A. Hayashi, and M. Tatsumisago, *Solid State Ionics*, 2016, ***285***, 79–82.
9 N. Kamaya, K. Homma, Y. Yamakawa, M. Hirayama, R. Kanno, M. Yonemura, T. Kamiyama, Y. Kato, S. Hama, K. Kawamoto, and A. Mitsui, *Nat. Mater.*, 2011, ***10***, 682–686.
10 A. Sakuda, A. Hayashi, and M. Tatsumisago, *Sci. Rep*., 2013, ***3***, 2261.
11 R. Mercier, J.P. Malgani, B. Fahys, and G. Robert, *Solid State Ionics*, 1981, ***5***, 663−666.
12 S. Ujiie, A. Hayashi, and M. Tatsumisago, *Solid State Ionics*, 2014, ***263***, 57−61.
13 H.-J. Deiseroth, S.-T. Kong, H. Eckert, J. Vannahme. C. Reiner, T. Zaiβ, and M. Schlosser, *Angew. Chem. Int. Ed*., 2008, ***47***, 755–758.
14 E. Rangasamy, Z. Liu, M. Gobet, K. Pilar, G. Sahu, W. Zhou, H. Wu, S. Greenbaum, and C. Liang, *J. Am. Chem. Soc.*, 2015, ***137(4)***, 1384−1387.
15 Z. Liu, W. Fu, E.A. Payzant, X. Yu, Z. Wu, N.J., Dudney, J. Kiggans, K. Hong, A.J. Rondinone, and C. Liang, *J. Am. Chem. Soc.* 2013, ***135***, 975–978.
16 S. Ito, M. Nakakita, Y. Aihara, T. Uehara, and N. Machida, *J. Power Sources*, 2014, ***271***, 342−345.
17 M. Uematsu, S. Yubuchi, K. Noi, A. Sakuda, A. Hayashi, and M. Tatsumisago, *Solid State Ionics*, 2018, ***320***, 33−37.
18 N.H.H. Phuc, K. Morikawa, M. Totani, H. Muto, and A. Matuda, *Solid State Ionics*, 2016, ***285***, 2−5.
19 N.H.H. Phuc, M. Totani, K. Morikawa, H. Muto, and A. Matuda, *Solid State Ionics*, 2016, ***288***, 240−243.
20 X. Yao, D. Liu, C. Wang, P. Long, G. Peng, Y.-S Hu, H. Li, L. Che, and X. Xu, *Nano Lett*., 2016, ***16***, 7148−7154.
21 S. Teragawa, K. Aso, K. Tadanaga, A. Hayashi, and M. Tatsumisago, *J. Mater. Chem. A*, 2014, ***2***, 5095–5099.
22 S. Yubuchi, A. Hayashi, and M. Tatsumisago, *Chem. Lett.*, 2015, ***44***, 884−886.
23 S. Yubuchi, S. Teragawa, K. Aso, K. Tadanaga, A. Hayashi, and M. Tatsumisago, *J. Power Sources*, 2015, ***293***, 941–945.
24 S. Yubuchi, M. Uematsu, M.K. Deguchi, A. Hayashi, and M. Tatsumisago, *ACS Appl. Energy Mater*., 2018, ***1(8)***, 3622−3629.
25 K.H. Park, D.Y. Oh, Y.E. Choi, Y.J. Nam, L. Han, J.-Y. Kim, H. Xin, F. Lin, S.M. Oh, and Y.S. Jung, *Adv. Mater*., 2016, ***28(9)***, 1874−1883.
26 Y.E. Choi, K.H. Park, D.H. Kim, D.Y. Oh, H.R. Kwak, Y.-G. Lee, and Y.S. Jung, *ChemSusChem* 2017, ***10(12)***, 2605−2611.
27 S.J. Sedlmaier, S. Indris, C. Dietrich, M. Yavuz, C. Dräger, F. Von Seggern, H. Sommer, and J. Janek, *J. Chem. Mater.* 2017, ***29(4)***, 1830−1835.
28 Y. Wang, Z. Liu, X. Zhu, Y. Tang, and F. Huang, *J. Power Sources*, 2013, ***224***, 225–229.
29 S. Boulineau, M. Courty, J.-M. Tarascon, and V. Viallet, *Solid State Ionics*, 2012, ***221***, 1–5.
30 M.A. Kraft, S.P. Culver, M. Calderon, F. Böcher, T. Krauskopf, A. Senyshyn, C. Dietrich, A. Zevalkink, J. Janek, and W.G. Zeier, *J. Am. Chem. Soc*., 2017, ***139(31)***, 10909−10918.
31 H.-J. Deiseroth, J. Maier, K. Weichert, V. Nickel, S.-T. Kong, and C. Reiner, *Anorg. Allg. Chem*., 2011, ***367***, 1287−1294.
32 D. H. Kim, D. Y. Oh, K. H. Park, Y. E. Choi, Y. J. Nam, H. A. Lee, S.-M. Lee, and Y. S. Jung, *Nano Lett*. 2017, ***17(5)***, 3013-3020.

33 N. Ohta, K. Takada, I. Sakaguchi, L. Zhang, R. Ma, K. Fukuda, M. Osada, and T. Sasaki, *Electrochem. Commun.* 2007, ***9***, 1486–1490.
34 F. Izumi and K. Momma, *Solid State Phenom.*, 2007, ***130***, 15−20.
35 T. Ozturk, E. Ertas, and O. Mert, *Chem. Rev.*, 2010, ***110***, 3419−3478.
36 A. Sakuda, T. Takeuchi, and H. Kobayashi, *Solid State Ionics* 2016, ***285***, 112−117.
37 A. Sakuda, A. Hayashi, T. Ohtomo, S. Hama, and M. Tatsumisago, *J. Power Sources*, 2011, ***196***, 6735–6741.
38 Y. Ito, S. Yamakawa, A. Hayashi, and M. Tatsumisago, *J. Mater. Chem. A*, 2017, ***5***, 10658–10668.
39 A. Sakuda, A. Hayashi, and M. Tastumisago, *Chem. Mater*., 2010, ***22(3)***, 949-956.

A table of contents entry

Graphic image

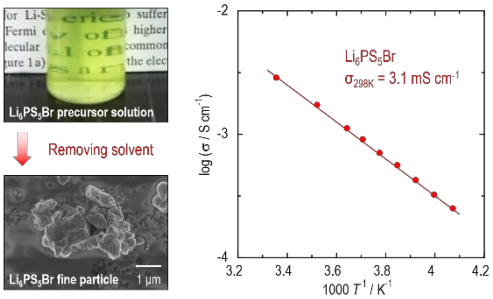

Sentence

Argyrodite Li_6PS_5Br electrolyte is synthesized using tetrahydrofuran and ethanol solvents and shows the highest conductivity of 3.1 mS cm^{-1}.